Ground-state properties of quasi-one-dimensional electron systems within dynamic local-field correction: Quantum Singwi-Tosi-Land-Sjölander theory

B. Tanatar
Department of Physics, Bilkent University, Bilkent, 06533 Ankara, Turkey

C. Bulutay
Department of Electrical and Computer Engineering, University of California, Santa Barbara, California 93106
and Department of Electrical and Electronics Engineering, Middle East Technical University, 06531 Ankara, Turkey

(Received 16 November 1998)

Dynamic local-field correction (LFC) brings a richer picture about the description of a many-body system than the standard mean-field theories. Here we investigate the ground-state properties of a quasi-one-dimensional electronic system using the quantum version of the Singwi-Tosi-Land-Sjölander (STLS) theory and present a critical account of its performance. The results are markedly different than those theories based on static LFC and the random-phase approximation; an example is the static structure factor, which develops a significant peak at low densities, signaling a developing ordered phase. An indication of growing instability at low densities is seen on $G(q,0)$, the static behavior of the dynamic LFC, which has an oscillatory character with a magnitude exceeding unity, peaking exactly at $4k_F$. The pair-correlation function comes out as positive for the densities considered in this work. The correlation energy and the compressibility curves are seen to be quite close to the static STLS results. A flaw of the theory is the significantly negative values of the dynamic structure factor around the plasmon frequencies, also the lifetime of the plasmons turns out to be negative away from the single-pair continuum. In summary, the major shortcomings of the dynamic STLS scheme are the violation of the compressibility sum rule (as in the static STLS case) and the misrepresentation of the plasmons in the dynamic structure factor. [S0163-1829(99)00324-0]

I. INTRODUCTION

Quantum confinement as in quasi-one-dimensional (Q1D) electronic systems, increases the role played by the many-body effects. As opposed to the Tomonaga-Luttinger liquid model[1,2] for the Q1D systems, Hu and Das Sarma[3] showed that in the presence of small disorder or finite temperature the Fermi surface is restored. This finding reassured the use of Fermi-liquid models[4] for characterizing Q1D systems. In particular, random-phase approximation (RPA)[4–6] and its improvements by including the static local-field correction (LFC), such as in the Singwi-Tosi-Land-Sjölander (STLS) approach[7] have been applied to Q1D systems.[8–13] Considering its performance in higher-dimensional systems as well, RPA is known to be successful in one-electron properties,[6] such as the self-energy and its end-products like band-gap renormalization and quasiparticle lifetime. Furthermore, the behavior of collective excitations (plasmons in this case) is seen to be quantitatively reproduced by RPA,[8] offering much better agreement with experiment[14] compared to its ''improved'' versions including LFC. However, from other many-body aspects, and in particular for the pair-correlation function, RPA gives grossly unphysical results,[7] which become worse as the dimensionality is reduced;[15] this artifact is directly carried over to the correlation energy results as well. In this regard, correlation energy functional of a many-body system happens to be an important input to the recent quantum freezing theories,[16,17] as has been demonstrated very recently on the estimation of Wigner crystallization density in quantum wires.[18] On the other hand, approaches having LFC such as STLS are successful in reproducing the pair-correlation function and correlation energy results of the quantum Monte Carlo (QMC) simulations from high densities to moderate densities; however, low-density performance is unsatisfactory,[19] and the violation of the compressibility sum rule over all densities is another problem shared with RPA.

A common viewpoint is the need to incorporate dynamical correlations to capture the full many-body physics. Specifically, the importance of dynamical local fields is evident from various applications such as construction of effective electron-electron interactions[20] that are relevant for Coulomb interaction induced superconductivity, electronic energy-loss straggling of protons in the electron gas,[21] determining the plasmon lifetime, and setting up the exchange-correlation potential in the context of time-dependent density-functional theory.[22] One of the pioneering works, offering a dynamic LFC is that of Hasegawa and Shimizu,[23] where they replaced the original STLS LFC scheme by a full quantum-mechanical framework with the use of Wigner distribution function. Their approach directly leads to a dynamic LFC and is usually named as the quantum STLS (QSTLS) or sometimes as the dynamic STLS. Later, Holas and Rahman reported a detailed numerical account of the QSTLS in three-dimensional (3D) electron liquid (EL),[24] Moudgil *et al.* applied QSTLS to 2D EL examining the spin-density response as well.[25] For the remaining Q1D EL, very recently we have investigated the performance of QSTLS, focusing mainly on the static properties.[26] Our aim in the present work is to bring the level of the current understanding about the performance of QSTLS to those of higher dimensions.[24,25] With this motivation, we give a critical account of the QSTLS in Q1D,

which we hope to be useful in the advancement of dynamic LFC schemes.

The outline of this paper is as follows. In Sec. II, we give the theoretical formalism of the self-consistent QSTLS equations, as well as the correlation energy and compressibility expressions. In Sec. III, we present the ground-state properties of the Q1D electronic systems using QSTLS theory, occasionally comparing with mainly the STLS results. In Sec. IV, we gather our assessment of the performance of the QSTLS for the Q1D electronic systems.

II. THEORETICAL FORMALISM

A. Self-consistent equations

The density response to a longitudinal perturbation coupled to density is governed by the longitudinal density-density response function, $\chi(q,\omega)$.[4] This quantity has central importance in characterizing a many-body system. The density-density response function beyond the RPA framework is usually taken to be of the form[27]

$$\chi(q,\omega)=\frac{\chi^0(q,\omega)}{1-U^0(q)[1-G(q,\omega)]\chi^0(q,\omega)}, \tag{1}$$

where $G(q,\omega)$ is the frequency- and wave-number-dependent LFC, representing the Pauli and Coulomb holes around each electron within the system, $\chi^0(q,\omega)$ is the density-density response function of the noninteracting system (here Q1D EL), $U^0(q)$ is the bare interaction potential for the Q1D EL. We model the Q1D EL as obtained from the zero-thickness 2D EL under a confining potential.[28] This yields $U^0(q)=(e^2/\epsilon_0)e^xK_0(x)$ for the Coulomb interaction between the electrons assumed to be in the lowest subband. Here $x=(bq/2)^2$, where b is the lateral width of the quantum wire determined by the confining oscillator frequency, and ϵ_0 is the background dielectric constant. The system is characterized by the dimensionless density parameter $r_s=a/a_B^*$, where a is the average interparticle distance (i.e., $n=1/2a$ in terms of the linear number density n), and $a_B^*=\epsilon_0/(m^*e^2)$ is the effective Bohr radius (we take $\hbar=1$). The single-subband approximation, which implies that the Fermi energy remains smaller than the intersubband energy difference, is justified for $r_s>(\pi/2^{5/2})(b/a_B^*)$. Since we have reported results for $b=2a_B^*$ only, in an earlier publication,[26] here we explore the dependence of various quantities on the width parameter. In this theoretical formalism section, we use normalized quantities for the wave number and energy, with the normalization being k_F (Fermi wave number) and $2E_F$ (E_F is the Fermi energy), respectively. We include disorder effects into our treatment within the simple number-conserving Mermin-Das scheme.[29] Accordingly, the density-density response function of the noninteracting system *with disorder* is given by

$$\chi^0_\gamma(q,\omega)=\frac{(\omega+i\gamma)\chi^0(q,\omega+i\gamma)}{\omega+i\gamma\dfrac{\chi^0(q,\omega+i\gamma)}{\chi^0(q,0)}}, \tag{2}$$

here γ is the disorder parameter, which we take throughout this work as 0.05 (in units of $2E_F$). For the dynamic LFC, the quantum version[23] of the original STLS approach[7] is used, which is given by

$$G(q,i\omega)=\frac{1}{4}\int_0^\infty dq'\frac{\chi^0_\gamma(q,q';i\omega)}{\chi^0_\gamma(q,i\omega)}\frac{U^0(q')}{U^0(q)}\times[S(q+q')-S(|q-q'|)]. \tag{3}$$

As in the 2D counterpart,[25] we work in the imaginary frequency formalism to facilitate the subsequent calculations. In Eq. (3), $\chi^0_\gamma(q,q';i\omega)$ is the inhomogeneous density-density response function given explicitly for the disorder-free case as

$$\chi^0(q,q';i\omega)=\frac{m^*}{\pi k_F}\frac{1}{q}\ln\left[\frac{\omega^2+\omega_-(q,q')^2}{\omega^2+\omega_+(q,q')^2}\right], \tag{4}$$

where m^* is the electron effective mass, and $\omega_\pm(q,q')=|q(1\pm q'/2)|$. For the expression of $\chi^0_\gamma(q,q';i\omega)$ with disorder, we similarly adapt Eq. (2) of the homogeneous case. $S(q)$ in Eq. (3) is the static structure factor, which is related to the density-density response function through the fluctuation-dissipation theorem as

$$S(q)=-\frac{1}{n\pi}\int_0^\infty d\omega\,\chi_\gamma(q,i\omega), \tag{5}$$

$$=-\frac{1}{n\pi}\int_0^\infty d\omega\frac{\chi^0_\gamma(q,i\omega)}{1-U^0(q)\chi^0_\gamma(q,i\omega)[1-G(q,i\omega)]}. \tag{6}$$

The primary advantage of analytic continuation of the response function to the complex frequency plane followed by Wick rotation of the frequency integral[30] is the robust capture of the plasmon contribution, which dominates in Q1D case. However, in its present form the integrand becomes slowly converging. As a remedy, to Eq. (5), we add and subtract the Hartree-Fock static structure factor

$$S_{\rm HF}(q)=\frac{1}{2\pi}\int_0^\infty d\omega\frac{1}{q}\ln\left[\frac{\omega^2+q^2(1-q/2)^2}{\omega^2+q^2(1+q/2)^2}\right] \tag{7}$$

with its closed form being $S_{\rm HF}(|q|<2)=|q|/2$ and $S_{\rm HF}(|q|>2)=1$, which then results in a rapidly decaying integrand.

Using $\lim_{\omega\to\infty}\chi^0(q,q';i\omega)/\chi^0(q,i\omega)=\lim_{\omega\to\infty}\chi^0(q,q';\omega)/\chi^0(q,\omega)=q'/q$, we get

$$\lim_{\omega\to\infty}G(q,i\omega)=G(q,i\infty)=G(q,\infty), \tag{8}$$

$$=\frac{1}{4}\int_0^\infty dq'\frac{q'}{q}\frac{U^0(q')}{U^0(q)}[S(q+q')-S(|q-q'|)]. \tag{9}$$

Note that $G(q,\infty)$ *formally* reduces to the expression satisfied by the STLS LFC, $G(q)$. Furthermore, the behavior for large ω is of the form $G(q,i\omega)=G(q,\infty)+\mathcal{O}(\omega^{-2})$. Based on this behavior, we compute $G(q,i\omega)$ up to a large value of ω (say ω_L) and then use for a value of $\omega>\omega_L$ the expression

$$G(q,i\omega)\simeq G(q,\infty)+\left(\frac{\omega_L}{\omega}\right)^2[G(q,i\omega_L)-G(q,\infty)]. \tag{10}$$

Equations (3) and (5) are to be solved self-consistently. Note that $G(q,i\omega)$ is real, whereas the dynamic LFC along the real frequency axis $G(q,\omega)$ is complex, which can be obtained from the former by the analytic continuation $i\omega\rightarrow\omega+i\eta$.

Finally, the pair-correlation function is the Fourier transform of the static structure factor

$$g(r)=1-\frac{1}{2}\int_0^\infty dq\cos(qr)[1-S(q)], \tag{11}$$

where, in the same spirit of normalization used throughout this section, distance r above is in units of $1/k_F$.

B. Correlation energy and compressibility

The correlation energy is the improvement in the ground-state energy of the many-body system over the Hartree-Fock estimate. The common approach is to calculate it via the coupling-constant integration.[6] The alternative is Rice's approach,[31] which has been revived recently,[32,13] where the correlation energy at a density r_s is given by

$$E_c(\mathrm{Ry}^*)=\frac{\pi}{32r_s^2}\int_0^\infty dq\int_0^\infty d\omega \times\left(\frac{\ln\{1-U^0(q)[1-G(q,i\omega)]\chi_\gamma^0(q,i\omega)\}}{1-G(q,i\omega)} + U^0(q)\chi_\gamma^0(q,i\omega)\right). \tag{12}$$

The exchange energy is given by

$$E_x(\mathrm{Ry}^*)=-\frac{1}{4r_s}\int_0^\infty dq\,F(q)[1-q/2], \tag{13}$$

where $F(q)=U^0(q)/(e^2/\epsilon_0)$. Both the exchange and correlation energy above are in 3D effective Rydberg units $[\mathrm{Ry}^*=m^*e^4/(2\epsilon_0^2)]$.

Isothermal compressibility is an important quantity as it challenges the approaches (including both RPA and STLS) via the compressibility sum rule. This sum rule requires the compressibility computed in two different ways to agree;[6] namely, compressibility is obtained by the second derivative of the energy and also by the long-wavelength behavior of the static dielectric function. In the former one, the inverse compressibility normalized to that of the noninteracting Fermi gas value (κ^0) is given by

$$\frac{\kappa^0}{\kappa}=1+\frac{8r_s^4}{\pi^2}\frac{d^2}{dr_s^2}[E_x(\mathrm{Ry}^*)+E_c(\mathrm{Ry}^*)], \tag{14}$$

whereas the alternative expression obtained via the long-wavelength static dielectric function, $\lim_{q\rightarrow0}\epsilon(q,0)$, leads to

$$\frac{\kappa^0}{\kappa}=1+\frac{4r_s}{\pi^2}\int_0^\infty dq\,F(q)\ln\left|\frac{2-q}{2+q}\right|\frac{dS(q)}{dq}. \tag{15}$$

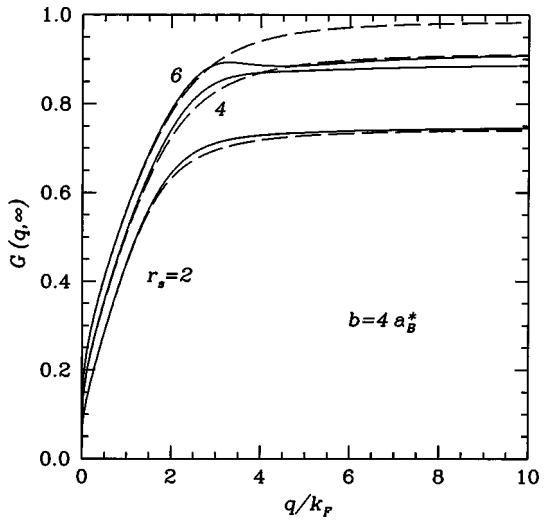

FIG. 1. Comparison of QSTLS $G(q,\infty)$ (solid lines) and STLS $G(q)$ (dashed lines) at $r_s=2$, 4, and 6, for a quantum wire of width $b=4\,a_B^*$.

III. RESULTS

A. Static properties

The expression for $G(q,\infty)$ is formally the same as that of the static STLS LFC, $G(q)$. However, the expressions for $S(q)$ in the static and dynamic cases are not the same, which renders $G(q,\infty)$ and $G(q)$ to be, in general, different due to the self-consistent nature of the equations. In Fig. 1 we compare these two quantities at several r_s values for a quantum wire of width $b=4\,a_B^*$. As seen, the discrepancy between the two increases with r_s. As the wire width increases, we need to go to larger values of r_s to fulfill the single-subband requirement. However, the low-density (large r_s) behavior is quite similar to the results obtained with other width parameters.[26] $S(q)$ results show similar characteristics, as asserted with the self-consistency requirements (cf. Fig. 2). It is observed that for $r_s\geqslant4$, $S(q)$ develops a single broad

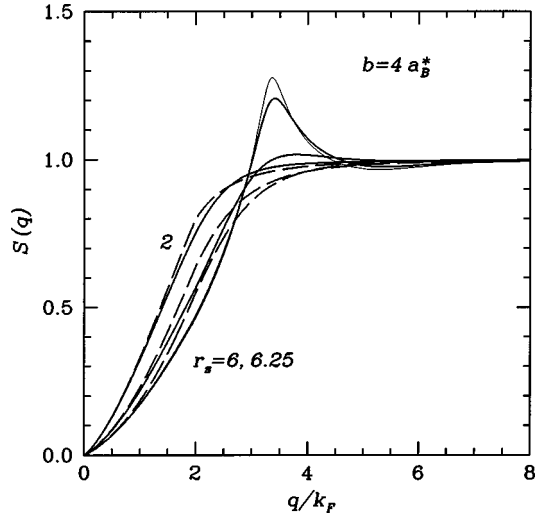

FIG. 2. Comparison of static structure factor for QSTLS (solid lines) and STLS (dashed lines) cases, at $r_s=2$, 4, and 6, for a quantum wire of width $b=4\,a_B^*$. The thin solid line is the QSTLS result for $r_s=6.25$.

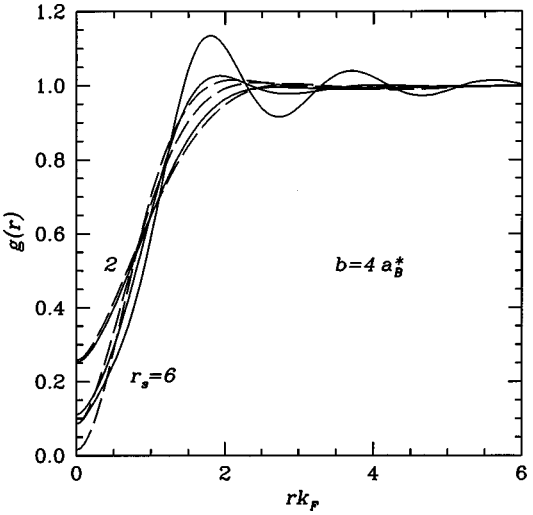

FIG. 3. Comparison of pair-correlation function for QSTLS (solid lines) and STLS (dashed lines) cases, at $r_s=2$, 4, and 6, for a quantum wire of width $b=4\,a_B^*$.

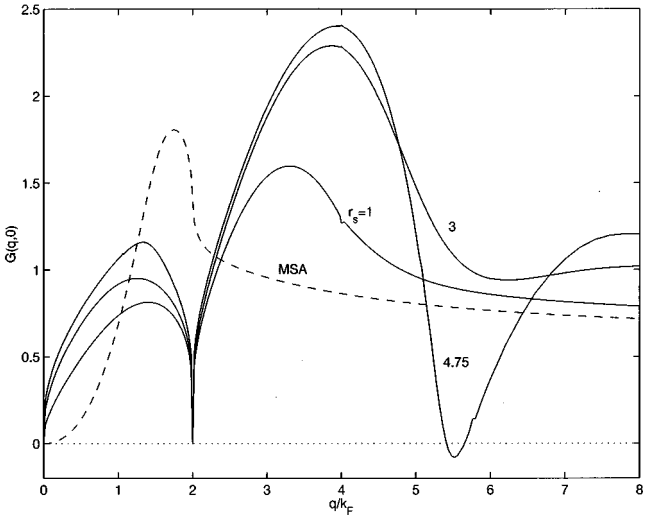

FIG. 4. The zero-frequency local-field factor $G(q,0)$ calculated using QSTLS (solid lines) for the indicated r_s values and $b=2\,a_B^*$; MSA result (dashed line) is also shown for $r_s=1$.

peak, which increases in magnitude; the static STLS theories,[11] as well as ladder approximation calculations,[33] do not produce an $S(q)$ with a marked peak for the same densities. In our case, we could achieve self-consistent solutions until $r_s\simeq 6.25$ (indicated by the thin solid line in Fig. 2). For $r_s=6.25$, the wave vector at which $S(q)$ is highly peaked $(3.4k_F)$, is somewhat close to the first star of the reciprocal lattice of a one-dimensional chain $(4k_F)$, which signals the evolution of an ordered structure. The peak in $S(q)$ occurs at $r_s=5$ for $b=2\,a_B^*$ quantum wires. This assertion is further supported by the recent prediction of Wigner crystallization densities of quantum wires,[18] estimating a value $r_s\simeq 5.7$ for a wire diameter of $2a_B^*$.

We show the STLS and QSTLS pair-correlation functions $[g(r)]$ in Fig. 3 for $r_s=2$, 4, and 6. For the densities of interest, $g(0)$ remains positive (a requirement severely violated by the RPA), with the QSTLS values being gradually higher than the STLS ones as r_s increases. $g(r)$ exhibits pronounced oscillatory behavior for the QSTLS case at $r_s=6$. QMC simulations and hypernetted-chain-type more sophisticated methods could be used to explore and test the behavior here. In general, our results show similar qualitative large r_s behavior for different wire widths. As would be expected, the indication of an ordered state occurs at a larger r_s value for wider quantum wires.

One of the most important figures of this work is Fig. 4, showing $G(q,0)$ for several r_s values, for a quantum wire of width $b=2\,a_B^*$. For all densities, $G(q,0)$ becomes zero[34] at $q=2k_F$ (in the disorder-free limit), which can be shown analytically[35] by considering Eq. (3) for $i\omega=0$ and $q=2k_F$. This peculiar behavior is common to the dynamic treatment of one-dimensional fermions, for the same result was also obtained by Nagano and Singwi[36] in their investigation of 1D fermions interacting via a repulsive δ-function potential. $G(q,0)$ shows at least two maxima, one around k_F and another at $4k_F$, the latter having a magnitude exceeding unity appreciably. Gasser[37] attributed the $4k_F$ instability in Q1D systems to multipair excitations. QSTLS does not include multipair excitations but surprisingly still signals a $4k_F$ instability, suggesting further research on this point. The oscillations in $G(q,0)$ grow to such an extent that for $r_s\simeq 4.75$ it becomes negative around $5.5k_F$; this may however be an artifact of the QSTLS. A noteworthy shortcoming of both the static and dynamic STLS theories is that the exact large q behavior[38] of the LFC is not reproduced. The QMC simulations of the response functions[39] in 2D and 3D EL indicate that the static LFC is an increasing function of q in contrast to the constant value attained in STLS approximations.[7,15,19] As shown by Holas,[38] discrepancy in the large q behavior is basically caused by approximating the true momentum distribution by its noninteracting counterpart.

To further test the origin of the sharp features in $G(q,0)$ around $2k_F$ and $4k_F$, we have repeated our self-consistent calculations using the response functions within the mean-spherical approximation (MSA).[40] In the MSA, the density-density response function takes the form

$$\chi^0_{\mathrm{MSA}}(q,\omega)=\frac{2n\epsilon_q}{\omega^2-[\epsilon_q/S_{\mathrm{HF}}(q)]^2+i\eta}, \tag{16}$$

where $\epsilon_q=q^2/2m^*$. Physically, the particle-hole continuum is approximated by a collective mode with Feynman-like energy spectrum $\epsilon_q/S_{\mathrm{HF}}(q)$. We have found that the use of χ^0_{MSA} in Eq. (3) removes the sharp features in $G(q,0)$ around $2\,k_F$ and $4\,k_F$ (cf. Fig. 4, where the MSA result at $r_s=1$ is indicated by the dashed line). This shows the importance of Fermi-liquid effects in the structure of $G(q,0)$.

B. Dynamic properties

The frequency dependence of the LFC is markedly different along the imaginary $(i\omega)$ and real (ω) frequency axes. Figure 5 reveals the weak frequency dependence of $G(q,i\omega)$ at several q values for $r_s=1$, which further justifies the use of imaginary frequency approach in self-consistent equations. The real and imaginary parts of $G(q,\omega)$ are contained in Fig. 6, displaying oscillatory dependence along the real

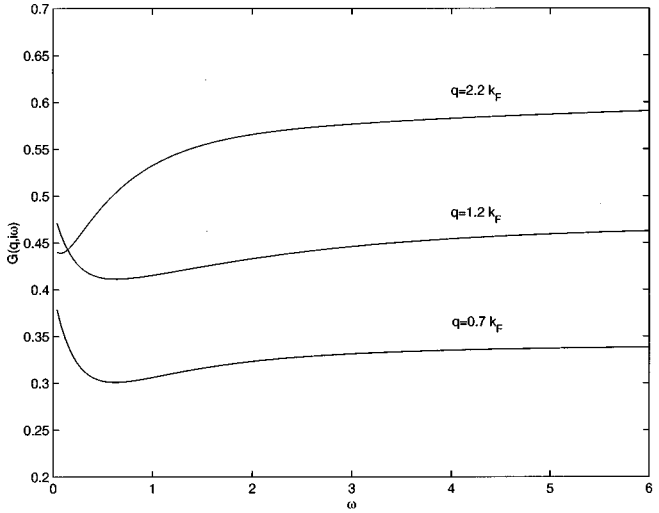

FIG. 5. The local-field factor evaluated on the imaginary frequency axis $G(q,i\omega)$, as a function of ω (in units of $2E_F$) for several q values at $r_s=1$. Quantum wire is of width $b=2\,a_B^*$.

frequency axis. The oscillatory trends in Figs. 5 and 6 are not specific to Q1D EL but were also observed in higher-dimensional electronic systems[24,25] and also in Bose liquids.[30] The results for two different r_s values shown in Fig. 6 indicate that the high-frequency limit of $\mathrm{Re}\,G(q,\omega)$ is density dependent. This observation is consistent with our earlier discussion of $G(q,\infty)$ in connection with the static properties. Similar behavior is also obtained for other values of the width parameter b.

Figure 7 shows a major flaw in the QSTLS theory, namely, the dynamic structure factor, $S(q,\omega)$, that becomes significantly negative for a single region of frequencies. This frequency region corresponds to the plasmon contribution, which is not in the form of a Dirac delta function, but broadened mainly due to finite disorder introduced into our computation. The negative contribution persists even in the zero-disorder ($\gamma=0$) case; thus, we are led to conclude that this violation of causality comes from the dynamic treatment of correlations. In the 2D counterpart,[25] the authors mention without giving a plot that $S(q,\omega)$ becomes slightly negative similar to the 3D case for frequencies beyond the upper edge of the electron-hole continuum. However, they do not establish any link with the misrepresentation of the plasmon contribution. In any case, the negative behavior of the dynamic structure factor in higher dimensions is not significant as in the Q1D case. This is also in compliance with our explanation, as the role of plasmons is especially enhanced in Q1D. The flaw may originate from the fact that, in the QSTLS, the dynamic nature of the LFC mainly comes from that of the Pauli hole. Thus, this imbalance between the Pauli and Coulomb hole dynamics may be instrumental here.

In this work, we have included the disorder effects in a phenomenological way through the parameter γ. We have confined ourselves to the weak disorder limit (typically, $\gamma \lesssim 0.1E_F$) and have not made a systematic study of the effects of higher values of γ. Small but finite γ renders the numerical computations somewhat smooth and allows us to use the Fermi-liquid theory as argued by Hu and Das Sarma.[3] The differences between the QSTLS and static STLS results are mostly due to the dynamic nature of the local-field factors. In

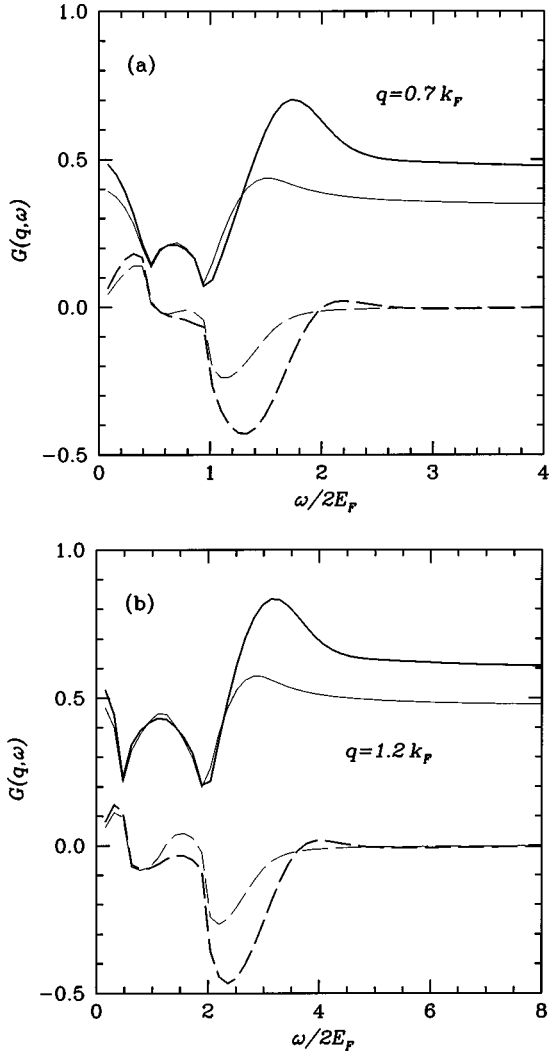

FIG. 6. $G(q,\omega)$ as a function of ω at $r_s=1$ (thin lines) and $r_s=3$ (thick lines); both real (solid lines) and imaginary (dashed lines) parts are displayed at $q=0.7k_F$ (a) and $q=1.2k_F$ (b). The quantum wire is of width $b=2\,a_B^*$.

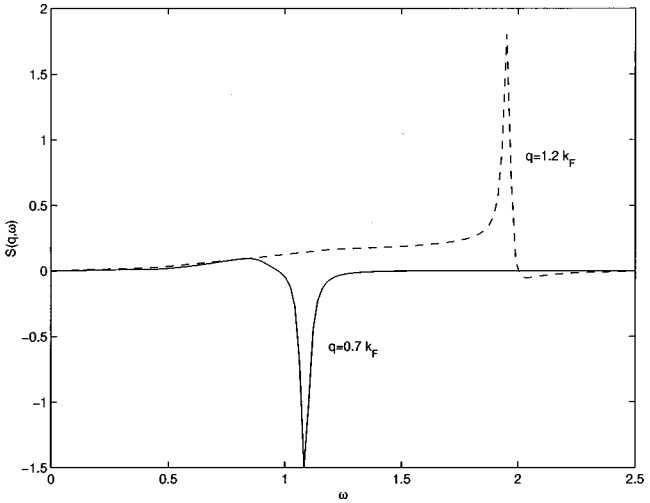

FIG. 7. $S(q,\omega)$ (in units of Fermi velocity) as a function of ω (in units of $2E_F$) for two q values at $r_s=1$. Quantum wire is of width $b=2\,a_B^*$.

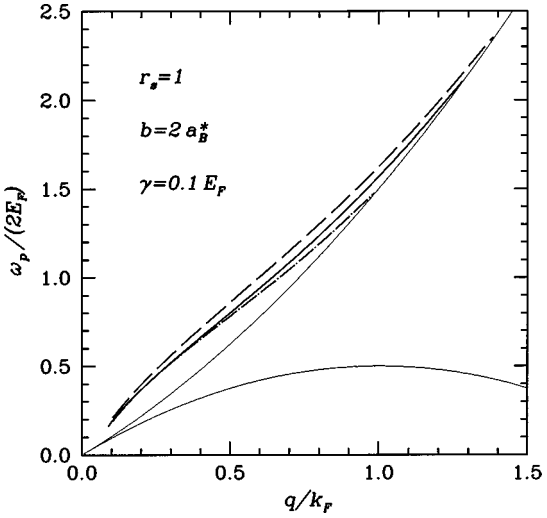

FIG. 8. Plasmon energy (in units of $2E_F$) as a function of q/k_F for QSTLS (solid), STLS (dash-dotted), and RPA (dashed) at $r_s=1$. Disorder parameter γ is taken as $0.1E_F$. Thin solid lines mark the boundary of the single-pair continuum. Quantum wire is of width $b=2\,a_B^*$.

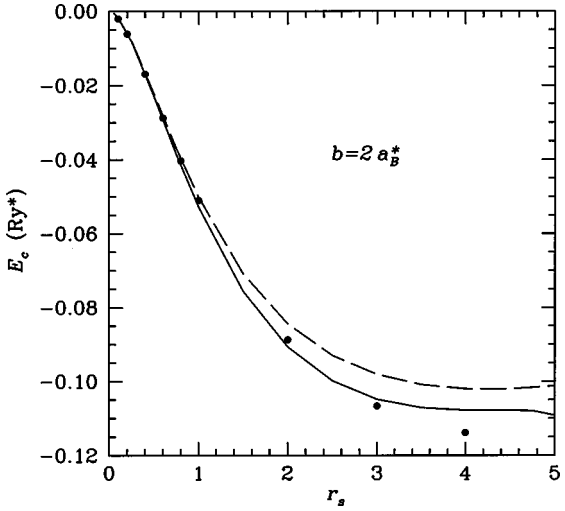

FIG. 9. Correlation energy (in 3D effective Rydbergs) as a function of r_s based on QSTLS (solid) and STLS (dashed), for $b=2\,a_B^*$. Solid circles are the results of Gold and Calmels (Ref. 11).

particular, the frequency dependence of real and imaginary parts of $G(q,\omega)$ are largely unaffected by the small amount of disorder included in our calculations. Disorder effects are most prominent in the long-wavelength behavior of plasmons, which are discussed below.

C. Plasmon dispersion and damping

The zeros of the dielectric function $\epsilon(q,\omega)$ determine the plasmon excitation spectrum (i.e., dispersion). In the case of dynamic LFC, the plasmons have a finite lifetime even outside the single-pair continuum. The excitation spectrum $\omega_p(q)$ and damping constant $\gamma_p(q)$ are determined by solving the complex-valued equation

$$1-U^0(q_p)[1-G(q_p,\omega_p-i\gamma_p)]\chi_\gamma^0(q_p,\omega_p-i\gamma_p)=0. \tag{17}$$

The results for the plasmon dispersion are shown in Fig. 8 at $r_s=1$, where QSTLS results fall between the RPA and STLS curves. This can be interpreted as an improvement over the STLS results, given the quantitative agreement of the RPA with experiment.[8,14] The finite disorder introduced into our computations leads to two effects: even in the RPA level, plasmons eventually enter into the single-pair continuum, also in the $q\to 0$ region the plasmons again suffer from damping, as reported previously by Das Sarma and Hwang.[10] Both in the disordered and zero-disorder cases the plasmon dispersions in the long-wavelength limit are the same for all approximations. In particular, the small q behavior of the plasmon dispersion is given by[41]

$$\omega_p\approx\frac{i}{2\tau}+\frac{1}{2}\left(4U^0(q)\frac{2q^2k_F}{\pi m}-\frac{1}{\tau^2}\right)^{1/2}, \tag{18}$$

in the presence of disorder, where $\tau=1/\gamma$ is the relaxation time. There exists a critical wave vector below which plasmons cannot propagate as discussed by Das[41] and recently by Das Sarma and Hwang.[10] The damping constant of the QSTLS theory comes out to be negative over a wide range of wave numbers, which rapidly switches to positive values as the dispersion curve approaches the single-pair continuum. The negative damping constant region can be matched directly with the negative values of the dynamic structure factor, indicating the fact that these two unphysical results have the same origin.

D. Correlation energy and compressibility

Correlation energy of the Q1D EL is computed using Rice's approach [Eq. (12)]. The results for the STLS and QSTLS are shown in Fig. 9. It is seen that QSTLS leads to a larger value (in magnitude) for the correlation energy, compared to STLS. We have not evaluated the correlation energy systematically for different values of the width parameter b, but surmise that similar trends will occur in those cases as well. There have been many calculations of the correlation energy E_c for a quantum wire employing different confinement models.[11–13] In Fig. 9 we compare our results with those of Gold and Calmels[11] who used the same quantum wire model to calculate the exchange-correlation energy and compressibility for different wire widths. Their results at low density lie below our static STLS curve, which may be due to their simplifying sum-rule approximation. The compressibility of the Q1D EL is computed in two different ways: using the second derivative of the exchange-correlation energy [Eq. (14)] and also using the long-wavelength limit of the static dielectric function [Eq. (15)]. STLS and QSTLS give very similar results and both still violate the compressibility sum rule (see Fig. 10). It could be possible to use the Vashishta-Singwi[42] theory to obtain better agreement for the compressibility sum rule.

IV. CONCLUSIONS

The advancement in the dielectric formulation of the many-body problem relies on the dynamic LFC schemes. A promising candidate in this respect is the QSTLS theory, and in this work we investigate its performance for the case of

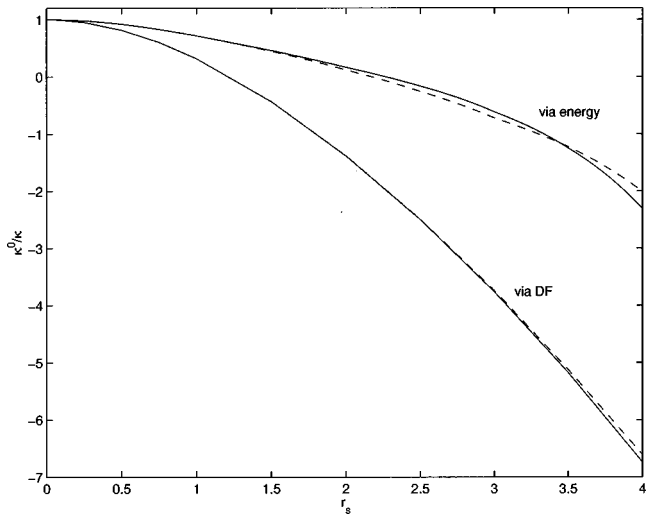

FIG. 10. Normalized inverse compressibility based on QSTLS (solid) and STLS (dashed), via the dielectric function and energy (see text), for $b=2\,a_B^*$.

Q1D EL. It is seen that QSTLS theory presents a remarkably different and richer picture compared to other mean-field theories such as STLS and RPA. Notably, the static structure factor develops a significant and narrow-width peak at $r_s \approx 6.25$ for $b=4\,a_B^*$. This finding is also in accordance with Wigner crystallization estimates[18] based on the quantum freezing theory. The static limit of the dynamic LFC $G(q,0)$ indicates an onset of a $4k_F$ density instability, towards $r_s=5$ value. The origin of this instability needs further investigation; however, we demonstrate the importance of the Fermi-liquid effects on the structure of $G(q,0)$. The correlation energy in the case of QSTLS is seen to be slightly larger, in magnitude, compared to the STLS results, whereas both approaches are very similar in the compressibility behaviors, both violating the compressibility sum rule.

A common experience established over the years in many-body physics is that a more involved approach does not necessarily lead to better results. This view is justified by QSTLS to some extent; the major drawback here, comes from the plasmon contribution to the dynamic structure factor, being reflected as negative, on the other hand, the plasmon dispersion of the QSTLS method falls in between the STLS and RPA curves. One possible culprit in the misrepresentation of the plasmons can be the dynamic LFC, which is mainly due to the dynamics of the Pauli hole. Other dynamic LFC schemes and also QMC simulations, which are currently lacking in Q1D case, will be very valuable in assessing the merits and flaws of the QSTLS approach.

ACKNOWLEDGMENTS

This work was supported by the Scientific and Technical Research Council of Turkey (TUBITAK) under Grant No. TBAG-1662. In the course of this work, C.B. was supported by TUBITAK-NATO. We thank Professor G. Senatore for fruitful discussions.

[1] S. Tomonaga, Prog. Theor. Phys. **5**, 544 (1950); J. M. Luttinger, J. Math. Phys. **4**, 1154 (1963).
[2] D. C. Mattis and E. H. Lieb, J. Math. Phys. **6**, 375 (1965); A. Luther and I. Peschel, Phys. Rev. B **9**, 2911 (1974); F. D. M. Haldane, J. Phys. C **14**, 2585 (1981).
[3] B. Y.-K. Hu and S. Das Sarma, Phys. Rev. B **48**, 5469 (1993).
[4] D. Pines and P. Nozières, *The Theory of Quantum Liquids* (Benjamin, New York, 1966), Vol. 1.
[5] A. L. Fetter and J. D. Walecka, *Quantum Theory of Many-Particle Systems* (McGraw-Hill, New York, 1971).
[6] G. D. Mahan, *Many-Particle Physics*, 2nd ed. (Plenum, New York, 1990).
[7] K. S. Singwi, M. P. Tosi, R. H. Land, and A. Sjölander, Phys. Rev. **179**, 589 (1968); K. S. Singwi and M. P. Tosi, Solid State Phys. **36**, 177 (1981).
[8] Q. P. Li and S. Das Sarma, Phys. Rev. B **40**, 5860 (1989); **41**, 10 268 (1990); **43**, 11 768 (1991).
[9] Q. P. Li, S. Das Sarma, and R. Joynt, Phys. Rev. B **45**, 13 713 (1992).
[10] S. Das Sarma and E. H. Hwang, Phys. Rev. B **54**, 1936 (1996).
[11] W. I. Friesen and B. Bergersen, J. Phys. C **13**, 6627 (1980); A. N. Borges, M. H. Degani, and O. Hipolito, Superlattices Microstruct. **13**, 375 (1993); A. Gold and L. Calmels, Solid State Commun. **100**, 137 (1996).
[12] L. Calmels and A. Gold, Phys. Rev. B **52**, 10 841 (1995); J. S. Thakur and D. Neilson, *ibid.* **56**, 4679 (1997).
[13] D. Agosti, F. Pederiva, E. Lipparini, and K. Takayanagi, Phys. Rev. B **57**, 14 869 (1998).
[14] A. R. Gõni, A. Pinczuk, J. S. Weiner, J. M. Calleja, B. S. Dennis, L. N. Pfeiffer, and K. W. West, Phys. Rev. Lett. **67**, 3298 (1991).
[15] M. Jonson, J. Phys. C **9**, 3055 (1976).
[16] S. Moroni and G. Senatore, Europhys. Lett. **16**, 373 (1991); C. N. Likos, S. Moroni, and G. Senatore, Phys. Rev. B **55**, 8867 (1997).
[17] A. R. Denton, P. Nielaba, and N. W. Ashcroft, J. Phys.: Condens. Matter **9**, 4061 (1997).
[18] B. Tanatar, I. Al-Hayek, and M. Tomak, Phys. Rev. B **58**, 9886 (1998).
[19] C. Bulutay and M. Tomak, Phys. Rev. B **53**, 7317 (1996).
[20] C. F. Richardson and N. W. Ashcroft, Phys. Rev. B **50**, 8170 (1994).
[21] N. P. Wang, J. Phys.: Condens. Matter **9**, 6837 (1997).
[22] J. F. Dobson, M. J. Bünner, and E. K. U. Gross, Phys. Rev. Lett. **79**, 1905 (1997).
[23] T. Hasegawa and M. Shimuzu, J. Phys. Soc. Jpn. **38**, 965 (1975).
[24] A. Holas and S. Rahman, Phys. Rev. B **35**, 2720 (1987); see also, H. K. Schweng and H. M. Böhm, *ibid.* **48**, 2037 (1993).
[25] R. K. Moudgil, P. K. Ahluwalia, and K. N. Pathak, Phys. Rev. B **52**, 11 945 (1995).
[26] C. Bulutay and B. Tanatar, Europhys. Lett. **43**, 572 (1998).
[27] See, for instance, J. T. Devreese, F. Brosens, and L. F. Lemmens, Phys. Rev. B **21**, 1349 (1980).
[28] G. Y. Hu and R. F. O'Connell, Phys. Rev. B **42**, 1290 (1990).
[29] N. D. Mermin, Phys. Rev. B **1**, 2362 (1970); A. K. Das, J. Phys. F **5**, 2035 (1975).

[30] K. Tankeshwar, B. Tanatar, and M. P. Tosi, Phys. Rev. B **57**, 8854 (1998).
[31] T. M. Rice, Ann. Phys. (N.Y.) **31**, 100 (1965).
[32] F. Pederiva, E. Lipparini, and K. Takayanagi, Europhys. Lett. **40**, 607 (1997).
[33] N. Nafari and B. Davoudi, Phys. Rev. B **57**, 2447 (1998); L. Calmels and A. Gold, *ibid.* **57**, 1436 (1998).
[34] In our previous work (Ref. 26), $G(q,0)$ had a dip at $q=2k_F$ without reaching zero value. This stemmed from using $\omega=0.02\,E_F$ value rather than $\omega=0$, due to numerical concerns in that computation. This is the reason for the minor discrepancy between $G(q,0)$ results presented here and in Ref. 26.
[35] The vanishing of $G(2k_F,0)$ can most easily be seen by considering the ratio $\chi^0(2k_F,k;0)/\chi^0(2k_F,0)$, which appears in the integrand [Eq. (3)]. At $q=2k_F$, the denominator tends to infinity while the numerator remains finite.
[36] S. Nagano and K. S. Singwi, Phys. Rev. B **27**, 6732 (1983).
[37] W. Gasser, Solid State Commun. **56**, 121 (1985).
[38] A. Holas, in *Strongly Coupled Plasma Physics*, edited by F. J. Rogers and H. E. DeWitt (Plenum, New York, 1987).
[39] S. Moroni, D. M. Ceperley, and G. Senatore, Phys. Rev. Lett. **69**, 1837 (1992); **75**, 689 (1995).
[40] See, for instance, N. Iwamoto, E. Krotscheck, and D. Pines, Phys. Rev. B **29**, 3936 (1984).
[41] A. K. Das, J. Phys. F **16**, L99 (1986).
[42] P. Vashishta and K. S. Singwi, Phys. Rev. B **6**, 875 (1972).